

Supporting Information

Sensitive, selective, and pretreatment-free detection of ferric ions in different solvents based on organic-soluble carbon dots

Jingfang Shangguan,^a Chengjie Qiao,^a Yuyang Zhang,^a Na Liu,^a Tongkun Wei,^a Zhuo Chen,^a Yuan Yuan,^a Qilu Li,^b Lin Li,^c Wei Liu^{a,*}

^a *School of Pharmacy, Xinxiang Medical University, Xinxiang, Henan 453003, China.*

^b *School of Environment, Henan Normal University, Key Laboratory for Yellow River and Huai River Water Environment and Pollution Control, Ministry of Education, Xinxiang, Henan 453007, China*

^c *School of Materials Science and Engineering, Suzhou University of Science and Technology, Suzhou 215009, P. R. China*

** Corresponding author: School of Pharmacy, Xinxiang Medical University, Xinxiang, Henan 453003, China;*

E-mail: liuwei@xxmu.edu.cn

Content

1. Table S1. The quantum yield (Φ) of CA-CDs under different synthesis conditions.
2. Figure S1. The particle size distribution of CA-CDs.
3. Figure S2. Normalized fluorescence emission spectra of CA-CDs at different excitation wavelengths.
4. Figure S3. Optimizing analytical conditions through variation of incubation time.
5. Figure S4. The fluorescence spectra of CA-CDs mixing with different organic solvents (10% v/v).
6. Table S2. The standard deviation (SD) of 20 blank samples.
7. Table S3. LOD verification by SNR (signal-to-noise ratio) method.
8. Figure S5. The selectivity of CA-CDs-based fluorescent sensor for Fe^{3+} detection in different solvents.
9. Figure S6. Image of CA-CDs incubation with different concentrations of Fe^{3+} and Cu^{2+} for 1 min.
10. Text S1. Photostability Evaluation of CA-CDs.
11. Table S4. Comparative analysis of analytical methods for Fe^{3+} determination in organic matrix.

Table S1. The quantum yield (Φ) of CA-CDs under different synthesis conditions.

Coffee acid (g)	Anhydrous ethanol (mL)	Temperature (°C)	Reaction durations (h)	$\Phi \pm \text{RSD}$
1.4	20	180	6	9.0% \pm 1.0%
1.6	20	180	6	8.9% \pm 0.2%
1.8	20	180	6	10.3% \pm 0.1%
2.0	20	180	6	9.9% \pm 0.9%
2.2	20	180	6	9.4% \pm 0.4%
2.4	20	180	6	9.1% \pm 0.1%
1.8	20	140	6	1.8% \pm 0.1%
1.8	20	160	6	3.9% \pm 0.4%
1.8	20	180	6	10.3% \pm 0.1%
1.8	20	200	6	13.8% \pm 0.3%
1.8	20	220	6	13.7% \pm 0.2%
1.8	20	200	2	11.5% \pm 0.8%
1.8	20	200	4	12.4% \pm 0.6%
1.8	20	200	6	13.8% \pm 0.3%
1.8	20	200	8	13.0% \pm 0.2%
1.8	20	200	10	12.9% \pm 0.2%

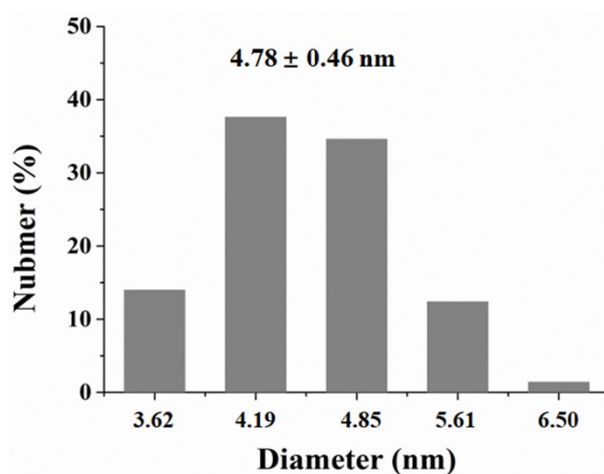


Figure S1. The particle size distribution of CA-CDs analyzed using dynamic light scattering.

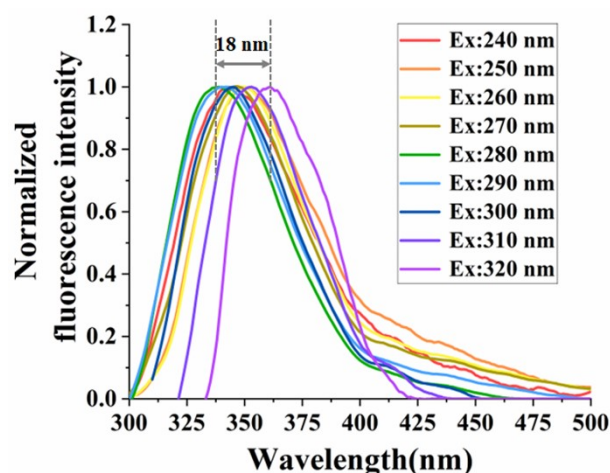


Figure S2. Normalized fluorescence emission spectra of CA-CDs at different excitation wavelengths.

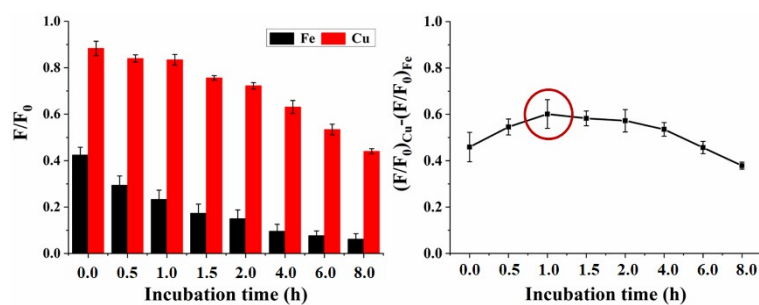


Figure S3. Optimizing analytical conditions through variation of incubation time. (A) The quenching efficiency of Fe^{3+} to CA-CDs at final concentration of $100 \mu\text{M}$ (black bar) and Cu^{2+} (red bar) various culture times. (B) the maximum value of the $\Delta(F/F_0)$ after CA-CDs incubating with Fe^{3+} and Cu^{2+} for varying durations.

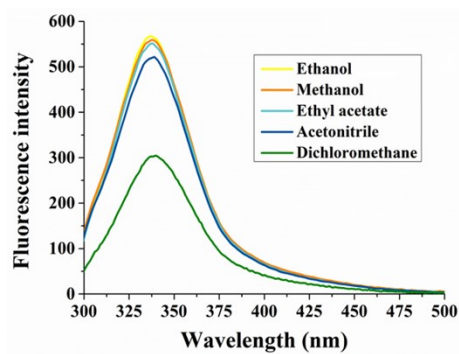


Figure S4. The fluorescence spectra of CA-CDs mixing with different organic solvents (10% v/v). The excitation wavelength was 290 nm.

Table S2. The standard deviation (SD) of 20 blank samples.

No. (blank)	F ₀ /F (EtOH)	F ₀ /F (MeOH)	F ₀ /F (EA)	F ₀ /F (ACN)	F ₀ /F (DCM)
1	1.0088	1.0014	1.0049	1.0012	1.0043
2	1.0036	0.9938	1.0194	0.9942	1.0129
3	0.9993	1.012	0.9972	1.0090	0.9983
4	0.9869	1.0023	0.9931	1.0037	0.9823
5	1.0103	1.0157	0.9822	1.0115	0.9968
6	1.0006	1.0004	1.0139	0.9979	1.0043
7	0.9976	0.9901	0.9957	0.9992	0.9996
8	0.9851	1.0140	1.0091	1.0034	1.0136
9	0.9887	0.9893	0.9908	0.9854	0.9825
10	0.9978	0.9900	0.9905	0.995	0.9963
11	0.9983	1.0033	0.9993	0.9981	1.0080
12	0.9965	0.9996	1.0012	1.0035	1.0105
13	0.9833	0.9899	0.9825	1.0112	0.9852
14	1.0096	1.0087	1.0013	0.9989	0.9992
15	1.0016	0.9998	1.0030	0.988	1.0079
16	0.9947	0.9903	1.0160	1.0153	0.9959
17	1.0194	0.999	0.9909	0.9964	1.0117
18	1.0035	1.0017	1.0047	1.0059	1.0026
19	1.0164	0.9971	1.0099	1.0120	1.0066
20	1.0021	1.0075	0.9859	1.0035	0.9822
SD value	0.0098	0.0083	0.0108	0.0079	0.0103

Note: (1) Abbreviations: EtOH (ethanol), MeOH (methanol), EA (ethyl acetate), ACN (acetonitrile), and DCM (dichloromethane), representing CA-CDs solutions mixed with each solvent at a 9:1 (v/v) ratio. (2) The excitation and emission wavelengths are 290 nm and 340 nm, respectively.

Table S3. LOD verification by SNR (signal-to-noise ratio) method.

Sample (signal)	LOD (μM)	Mean (F_0/F)	SNR value
EtOH	0.96	1.0337 ± 0.0259	3.44
MeOH	1.66	1.0415 ± 0.0314	6.20
EA	1.54	1.0438 ± 0.0176	3.98
ACN	1.72	1.0339 ± 0.0215	3.49
DCM	1.19	1.0453 ± 0.0603	4.40

Note: (1) Abbreviations: EtOH (ethanol), MeOH (methanol), EA (ethyl acetate), ACN (acetonitrile), and DCM (dichloromethane), representing CA-CDs solutions mixed with each solvent at a 9:1 (v/v) ratio. (2) The excitation and emission wavelengths are 290 nm and 340 nm, respectively. (3) SNR value was calculated by equation:

$$\text{SNR} = \frac{\text{Mean (Signal)} - \text{Mean (blank)}}{\text{SD value (blank)}}$$

where the “Mean (blank)” and “SD value (blank)” is the average values and standard deviation values of 20 blank samples, respectively.

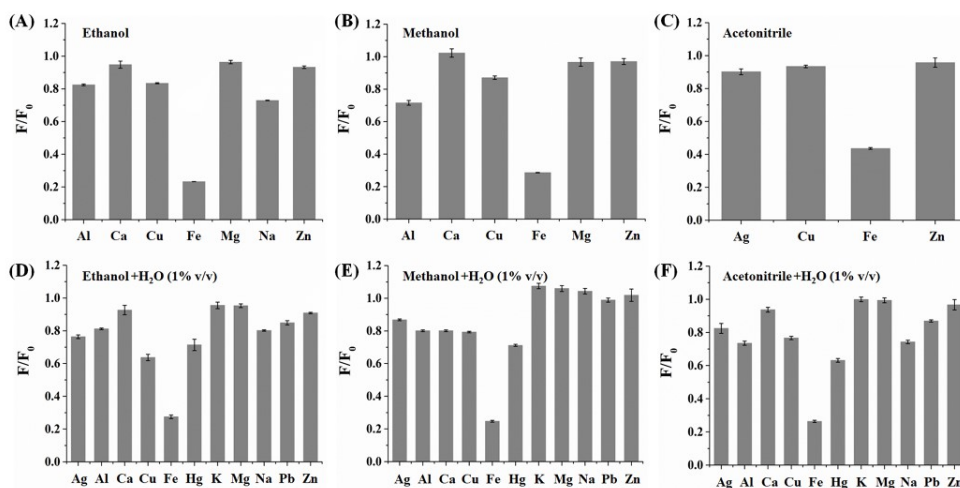


Figure S5. The selectivity of CA-CDs-based fluorescent sensor for Fe³⁺ detection in different solvents. The final concentration of all metal ion is 100 μM .

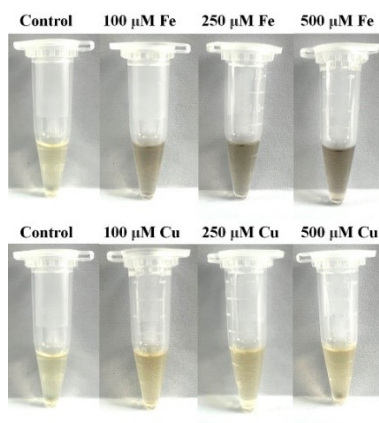


Figure S6. Image of CA-CDs incubation with different concentrations of Fe³⁺ and Cu²⁺ for 1 min.

Text S1. Photostability Evaluation of CA-CDs

The photostability of CA-CDs was evaluated using an RF-6000 spectrophotometer (Shimadzu, Japan) equipped with a 150 W steady-state xenon lamp (power density is approximately 160 mW/cm²). To investigate the effect of environmental temperature, CA-CDs solution mixed with different solvents (ethanol, methanol, ethyl acetate, acetonitrile, and dichloromethane; 9:1, v/v) were incubated at 4°C, 25°C, and 35°C prior to fluorescence measurement. For photobleaching behavior analysis, these five CA-CDs solutions were continuously irradiated for 2 h under characteristic wavelength excitation. Additionally, their photostability was monitored under indoor LED white light (40 W power, 2.5 m from light source) a period of 30 days, with eight-hour daily illumination. All measurements were performed in triplicate. The excitation and emission wavelengths were set to 290 nm and 340 nm, respectively, with bandwidths of 1.5 nm (excitation) and 3.0 nm (emission), and scanning sensitivity was set in "auto" mode.

Table S4. Comparative analysis of analytical methods for Fe³⁺ determination in organic matrix.

Method	Method of sample preparation	Time Taken	Instrument Required	LOD	Test sample	Reference
UV-Vis	Ashing and acid digestion	7.5 h	UV-Vis spectrophotometer	304.4 µM	crude oil	1
FAAS	Direct introduction	Not specified	FAAS coupled with multicommutation flow process	0.011 µM	lubricating oils	2
	Preconcentration and extraction	40 min (excluding extraction)	FA-FAAS (Fast sequence flame atomic absorption spectrometry)	0.039 µM	gasoline	3
ICP-OES	Deep eutectic solvent-based extraction	45 min	ICP-OES	0.02 mg/kg	vegetable oil, motor oil	4
	Direct introduction	Few minutes	ICP-OES coupled to an ultrasonic nebulizer with a membrane for desolvation	0.20 µg/kg	fuel ethanol	5
	Hot solvent extraction	40 min	ICP-OES	0.0047 µM	crude oil	6
ICP-AES	Dissolved in DMF/EDTA diluent	Not specified	ICP- AES coupled with a membrane desolvation unit	0.02 µM	active pharmaceutical samples	7

XRF	Homogenization and dilution	15 min	Energy dispersive XRF	2.2 $\mu\text{g/g}$	crude oil	8
	Distillation	20 min	energy dispersive XRF	0.27 μM	gasoline	9
MP-AES	Dissolved in o-xylene diluent	30 min	MP-AES	0.01 mg/kg	crude oil	10
FS	Direct introduction after incubation	less than 10 min	fluorescence spectrophotometry	50 μM	gasoline	11
	Direct introduction after incubation	over 12 h	fluorescence spectrophotometry	5.10 μM	MeOH	12
	Direct introduction after incubation	1 h	fluorescence spectrophotometry	0.96 – 2.82 μM	EtOH, MeOH, EA, ACN, DCM, ethanol gasoline	This work

Note: (1) Abbreviations: UV-Vis (Ultraviolet–Visible Spectroscopy), FAAS (Flame Atomic Absorption Spectroscopy), ICP-OES (Inductively Coupled Plasma Optical Emission Spectrometry), XRF (X-ray Fluorescence Spectroscopy), MP-AES (Microwave Plasma Atomic Emission Spectroscopy), FS (Fluorescence Spectroscopy), EtOH (ethanol), MeOH (methanol), EA (ethyl acetate), ACN (acetonitrile), and DCM (dichloromethane).

(2) All Detection of Limit (LOD) values reported in “mass/volume” units in the reference were converted to molar concentrations (μM) to facilitate comparison.

Reference:

1. A. B. Shehata, G. G. Mohamed, M. A. Gab-Allah. Simple Spectrophotometric Method for Determination of Iron in Crude Oil. *Petroleum Chemistry*, 2017, **57**, 1007–1011. DOI: 10.1134/S096554411712012X
2. B. F. Reis, M. Knochen, G. Pignalosa, N. Cabrera, J. Giglio. A multicommuted flow system for the determination of copper, chromium, iron and lead in lubricating oils with detection by flame AAS. *Talanta*, 2004, **64**, 1220 - 1225. DOI:10.1016/j.talanta.2004.03.070
3. D. S. S. Santos, M. G. A. Korn, M. A. B. Guida, G. L. D. Santos, V. A. Lemos, L. S. G. Teixeira. Determination of Copper, Iron, Lead and Zinc in Gasoline by Sequential Multi-Element Flame Atomic Absorption Spectrometry after Solid Phase Extraction. *J. Braz. Chem. Soc.*, 2011, **22**, 552 - 557. 10.1590/s0103-50532011000300020
4. A. Shishov, S. Savinov, N. Volodina, I. Gurev, A. Bulatov. Deep eutectic solvent-based extraction of metals from oil samples for elemental analysis by ICP-OES. *Microchemical Journal*, 2022, **179**, 107456. <https://doi.org/10.1016/j.microc.2022.107456>
5. M. S. Rocha, M. F. Mesko, F. F. Silva, R. C. Sena, M. C. B. Quaresma, T. O. Araújo, L. A. Reis. Determination of Cu and Fe in fuel ethanol by ICP-OES using direct sample introduction by an ultrasonic nebulizer and membrane desolvator. *J. Anal. At. Spectrom.*, 2011, **26**, 456 - 461. <https://doi.org/10.1039/C0JA00096E>
6. M. D. O. Souza, M. A. Ribeiro, W. D. C. M. Tereza, G. P. Brandao Athayde, R. D. C. E. Vinicius, F. D. S. F. Luan, et al. Evaluation and determination of chloride in crude oil based on the counterions Na, Ca, Mg, Sr and Fe, quantified via ICP-OES in the crude oil aqueous extract. *Fuel*, **154**, 181-187. <http://dx.doi.org/10.1016/j.fuel.2015.03.079>
7. Q. Tu, T. Wang, V. Antonucci. High-efficiency sample preparation with dimethylformamide for multi-element determination in pharmaceutical materials by ICP-AES. *Journal of Pharmaceutical and Biomedical Analysis*, 2010, **52**, 311 - 315. <https://doi.org/10.1016/j.jpba.2010.01.008>

8. A. Doyle, A. Saavedra, M. L. B. Tristão, R. Q. Aucelio. Determination of S, Ca, Fe, Ni and V in crude oil by energy dispersive X-ray fluorescence spectrometry using direct sampling on paper substrate. *Fuel*, 2015, **162**, 39–46.
<https://doi.org/10.1016/j.fuel.2015.08.072>
9. L. S. G. Teixeira, R. B. S. Rocha, E. V. Sobrinho, P. R. B. Guimarães, L. A. M. Pontes, J. S. R. Teixeira. Simultaneous determination of copper and iron in automotive gasoline by X-ray fluorescence after pre-concentration on cellulose paper. *Talanta*, 2007, **72**, 1073 - 1076.
<https://doi.org/10.1016/j.talanta.2006.12.042>
10. J. Nelson, G. Gilleland, L. Poirier, D. Leong, P. Hajdu, F. Lopez-Linares. Elemental Analysis of Crude Oils Using Microwave Plasma Atomic Emission Spectroscopy. *Energy Fuels*, 2015, **29**, 5587–5594. DOI: 10.1021/acs.energyfuels.5b01026
11. Y. He, Z. Feng, X. Shi, S. Li, Y. Liu, G. Zeng, H. He. N- and O-Doped Carbon Dots for Rapid and High-Throughput Dual Detection of Trace Amounts of Iron in Water and Organic Phases. *Journal of Fluorescence*, 2019, 29, 137 – 144.
<https://doi.org/10.1007/s10895-018-2321-5>
12. L. He, C. Liu, J. H. Xin. A novel turn-on colorimetric and fluorescent sensor for Fe³⁺ and Al³⁺ with solvent-dependent binding properties and its sequential response to carbonate. *Sensors and Actuators B*, 2015, 213, 181 - 187.
<http://dx.doi.org/10.1016/j.snb.2015.02.060>